Elastic properties of pyrolytic carbon with axisymmetric textures

T. Böhlke, K. Jöchen, R. Piat, T.-A. Langhoff, I. Tsukrov, B. Reznik

In this paper, the first-order bounds, the geometric mean, the singular approximation and the self-consistent estimate of the linear elastic properties of pyrolytic carbon (PyC) are determined numerically. The texture, i.e. the orientation distribution of the normal direction of the graphene planes, is modeled by a Fisher distribution on the unit sphere. Fisher distributions depend only on one scalar concentration parameter. It is shown in detail how the effective elasticities of PyC can be estimated based on the one concentration parameter which describes the scatter width of the orientation distribution. The numerical predictions of the different bounds and estimates are compared.

1 Introduction

Pyrolytic carbon (PyC) is commonly used as micro constituent of carbon/carbon or carbon/silicon carbide composites. Because of their excellent mechanical properties at high temperatures, these composites find several applications as aircraft, aerospace, car and nuclear fuel rod components. Examples of such superior properties of these materials are the increase of Young's modulus and the thermal conductivity in the high temperature range up to 2000°C (Fitzer and Manocha, 1998; Herbell and Eckel, 1991).

In order to understand the macroscopic material properties one has to investigate the microstructure of PyC. This can be performed, e.g., by coupling experimental characterization methods like transmission electron microscopy (TEM) with selected-area electron diffraction (SAED) (Reznik et al., 2003). On the submicron scale the microstructure of PyC can be described as a set of coherent domains having different preferred orientations or textures in relation to the fiber surface (or to the surface of the plane substrate), which are classified as: isotropic, low-textured (LT), medium-textured (MT) and high-textured (HT), see, e.g., Fig. 1 (Reznik et al., 2001; Reznik and Hüttinger, 2002). Each domain in Fig. 1 (a, b) represents the two-dimensional cross section of the three-dimensional stack of graphene planes. Different degrees of texture induce different material properties. Guellali et al. (2008a,b) provide a very accurate description (SEM, light microscopy) and experimental characterisation (X-ray diffraction, three point bending tests) of differently textured PyCs including information about typical spacing between graphene planes, apparent stack height, effective elastic modulus and other properties.

In this contribution, we restrict ourselves to PyC produced by chemical vapour infiltration. In this case, the growth process of the PyC matrix around the fibers is uniform with an approximate rotational symmetry in normal direction to the fiber surface. A typical microstructure of such a composite is presented in Fig. 1 (c). The PyC layers are parallel to the fiber surface. Several experimental methods have been used for measuring the elastic properties of PyC. Among them are ultrasonic pulse-echo experiments (Papadakis and Bernstein, 1963) and sharp indentation tests (Diss et al., 2002), but due to the significant anisotropy of PyC only quasi-effective properties of the material were obtained by these tests. Alternatively, numerical approaches for computing the elastic properties of PyC have been reported (Piat et al., 2004; Sauder and Lamon, 2005; Sauder et al., 2005).

Crystallographic textures can often be described by a small number of texture components (Bunge, 1993; Kocks et al., 1998). A texture component is a crystal or domain orientation for which the orientation distribution function (ODF) shows a (local) maximum. In the neighborhood, the ODF is decreasing in an isotropic or anisotropic way. In the present paper, we model the orientation distribution of domains by a simple one-parameter axial orientation distribution function. More specifically, we describe the microtexture in PyC by a Fisher distribution and determine the elastic properties of PyC on the microscale numerically by different submicron-to-mirco scale transition schemes. The Fisher distribution describes a Gauss type distribution of normal vectors, which determine the orientation of the domains. Since on unit spheres there exist no normal distributions (Schaeben, 1990, 1992), e.g., Fisher distributions can be considered (Fisher, 1953). The main result of the paper is to show, how the elastic
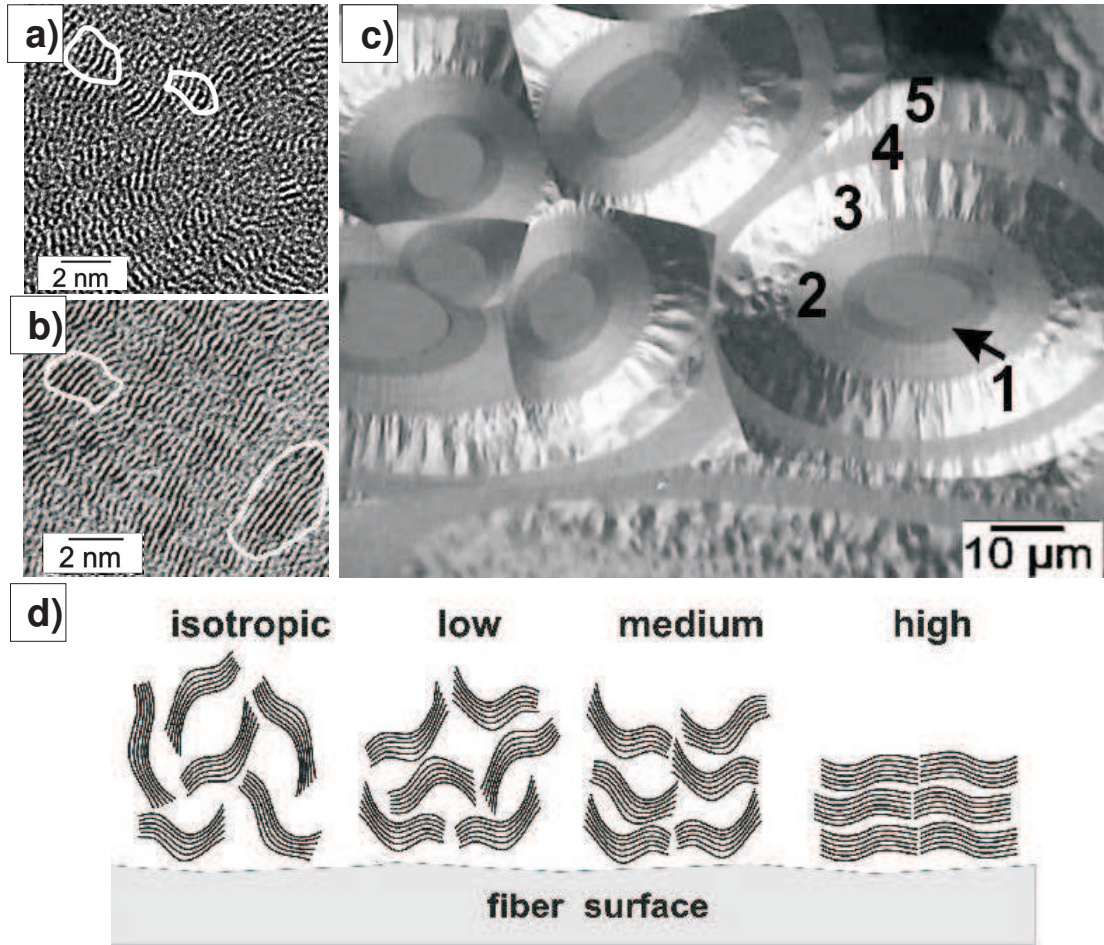
Figure 1: High resolution TEM images of the typical a) medium textured (MT) and b) high textured (HT) coherent domains; c) polarized light micrograph of a polished section of an infiltrated carbon fiber felt with differently textured PyC layers (1-5) and d) schematics of different layer textures

parameters on the microscale of PyC depend on the single concentration parameter which specifies completely the Fisher distribution. For the homogenization of the elastic properties the first-order bounds, the geometric mean, the singular approximation and the self-consistent estimate are determined. The computational procedure is discussed in detail for the singular approximation, which is shown to be very close to the geometric mean and the self-consistent estimate for spherical domains. In contrast to the geometric mean the singular approximation is based on clear mechanical assumptions. Compared to the self-consistent estimate, the determination of the singular approximation is much simpler.

The outline of the paper is as follows. In the first part of the paper, the orientation distribution function of graphene planes is modeled by a Fisher distribution. Then, different bounds and estimates for the elastic properties of PyC on the submicron scale are discussed. In the last part of the paper, the bounds and estimates are determined numerically for microtextures exhibiting axisymmetric textures with different concentrations.

Notation. A direct tensor notation is preferred throughout the text. If tensor components are used, then the Einstein summation convention is applied. Vectors and 2nd-order tensors are denoted by lowercase and uppercase bold letters, e.g., a and A, respectively. A linear mapping of 2nd-order tensors by a 4th-order tensor is written as $A = \mathbb{C}[B]$. The scalar product and the dyadic product are denoted, e.g., by $a \cdot b$ and $a \otimes b$, respectively. The composition of two 2nd-order or two 4th-order tensors is formulated by AB and $\mathbb{AB}$. We define $(A \square B)[C] = ACB \; \forall A, B, C$ and $(a \otimes b) \cdot (\mathbb{C}[[a \otimes b]]) = (a \otimes a) \cdot (\mathbb{C}[b \otimes b]) \; \forall a, b, \mathbb{C}$. Completely symmetric and traceless tensors are designated by a prime, e.g., A'. The brackets $\langle \cdot \rangle$, e.g., $\langle \varepsilon \rangle$, indicate ensemble averaging which for ergodic media can be identified with volume averages in the infinite volume limit. The symbol $\star$ denotes the Rayleigh product, which for tensors $\mathbb{T} = T_{ij...l} \, e_i \otimes e_j \otimes \ldots \otimes e_l$ of arbitrary rank

is defined by $\boldsymbol{Q} \star \mathbb{T} = T_{ij\ldots l}(\boldsymbol{Q}\boldsymbol{e}_i) \otimes (\boldsymbol{Q}\boldsymbol{e}_j) \otimes \ldots \otimes (\boldsymbol{Q}\boldsymbol{e}_l)$. The product $\boldsymbol{Q} \star \mathbb{T}$ can be interpreted as the rotation of the tensor $\mathbb{T}$ by the orthogonal tensor $\boldsymbol{Q}$. The tensor $\boldsymbol{I}$ is the identity on vectors. The identity on symmetric 2nd-order tensors is denoted by $\mathbb{I}^S$. $\mathbb{A}^{\mathsf{T}_\mathsf{R}}$ indicates the right minor transposition of $\mathbb{A}$, which satisfies $\boldsymbol{A} \cdot (\mathbb{A}[\boldsymbol{B}]) = \boldsymbol{A} \cdot (\mathbb{A}^{\mathsf{T}_\mathsf{R}}[\boldsymbol{B}^\mathsf{T}]) \; \forall \boldsymbol{A}, \boldsymbol{B}$.

2 Crystallographic texture

Orientation distribution function of graphene planes. The orientation of a domain can be described approximately by a normal vector $\boldsymbol{c}$ perpendicular to the graphene planes, or equivalently by a proper orthogonal tensor $\boldsymbol{Q} \in SO(3)$

$$\boldsymbol{c} = \boldsymbol{Q}\boldsymbol{c}_0, \tag{1}$$

where $\boldsymbol{c}_0$ is an arbitrary but constant reference vector. It should be noted that for given $\boldsymbol{c}$ and fixed $\boldsymbol{c}_0$ the tensor $\boldsymbol{Q}$ is not unique since arbitrary rotations about $\boldsymbol{c}_0$ or $\boldsymbol{c}$ are not relevant. Hence, $\boldsymbol{Q}$ can be specified by two independent parameters only. This will be taken into account by the specific structure of the distribution function introduced later on. The orientation distribution function of graphene planes $f_c(\boldsymbol{c})$ specifies the volume fraction $\mathrm{d}v/v$ of domains with the orientation $\boldsymbol{c}$, i.e.,

$$\frac{\mathrm{d}v}{v}(\boldsymbol{c}) = f_c(\boldsymbol{c})\,\mathrm{d}c, \tag{2}$$

where $\mathrm{d}c$ is the surface element of the unit sphere $\mathcal{S}^2$ in the three-dimensional Euclidean space. The ODF can be described equivalently by a distribution function $f(\boldsymbol{Q})$ specifying the volume fraction $\mathrm{d}v/v$ of domains with the orientation $\boldsymbol{Q}$, i.e.,

$$\frac{\mathrm{d}v}{v}(\boldsymbol{Q}) = f(\boldsymbol{Q})\,\mathrm{d}Q. \tag{3}$$

Here, $\mathrm{d}Q$ is the volume element in $SO(3)$ which ensures an invariant integration over $SO(3)$. The function $f(\boldsymbol{Q})$ is nonnegative and normalized $\int_{SO(3)} f(\boldsymbol{Q})\,\mathrm{d}Q = 1$. The orientation distribution function $f(\boldsymbol{Q})$ reflects both, the material symmetry of the domains forming the aggregate and the symmetry of the microstructure. The material symmetry of the domains implies the following symmetry relation: $f(\boldsymbol{Q}) = f(\boldsymbol{Q}\boldsymbol{H}^D) \; \forall \boldsymbol{H}^D \in S^D \subseteq SO(3)$, where S^D denotes the material symmetry group. The domains are assumed to have a transversely isotropic symmetry. The symmetry of the microstructure implies $f(\boldsymbol{Q}) = f(\boldsymbol{H}^M \boldsymbol{Q}) \; \forall \boldsymbol{H}^M \in S^M \subseteq SO(3)$, where S^M denotes the symmetry group of the microstructure, i.e., the considered volume element on the submicron scale. The functions f and f_c are related by

$$f(\boldsymbol{Q}) = f_c(\boldsymbol{Q}\boldsymbol{c}_0). \tag{4}$$

Fisher distributions. For simplicity we model the orientation distribution of domains given by the $\boldsymbol{c}$ axes based on a one-parameter axial orientation distribution function. Based on the central limit theorem, any finite sum of independent and identically distributed random numbers in Euclidean space can be approximated by a Gaussian distribution. However, no simple analogue for the central limit theorem for hyperspheres exists (Schaeben, 1990, 1992), but for the purpose of mathematical statistics the analogue of the Gauss normal distribution in case of hyperspheres $\mathcal{S}^p$ are the von-Mises-Fisher distributions (and in the case $p = 3$ the Fisher distributions) (Fisher, 1953). Thus, we can use Fisher distributions for modeling the orientation of the unit normal vectors of the graphene planes. Their probability function has the general form

$$f_c(\boldsymbol{c}) = \frac{\kappa}{\sinh(\kappa)} \exp(\kappa\,\bar{\boldsymbol{c}} \cdot \boldsymbol{c}), \tag{5}$$

where the vector $\bar{\boldsymbol{c}}$ is the mean direction or expectation value of the distribution being rotationally symmetric around $\bar{\boldsymbol{c}}$ whereas κ is the so-called concentration parameter. For $\kappa = 0$ the distribution is uniform. It should be noted that the function f_c is not even, i.e., $f_c(\boldsymbol{c}) \neq f_c(-\boldsymbol{c})$. Since the considered distributions of graphene planes are axial distributions, the ansatz is modified as follows

$$f_c(\boldsymbol{c}) = \frac{1}{2}\frac{\kappa}{\sinh(\kappa)} \left(\exp(\kappa\,\bar{\boldsymbol{c}} \cdot \boldsymbol{c}) + \exp(-\kappa\,\bar{\boldsymbol{c}} \cdot \boldsymbol{c})\right), \tag{6}$$

If the function f is used instead of f_c one derives from (6)

$$f(\boldsymbol{Q}) = \frac{1}{2}\frac{\kappa}{\sinh(\kappa)} \left(\exp(\kappa\bar{\boldsymbol{c}} \cdot (\boldsymbol{Q}\boldsymbol{c}_0)) + \exp(-\kappa\bar{\boldsymbol{c}} \cdot (\boldsymbol{Q}\boldsymbol{c}_0))\right). \tag{7}$$

The unit normal $\boldsymbol{c}$ on each graphene plane can be represented by its endpoint on the sphere around the center $\mathcal{O}$ and thus be described by spherical coordinates $\{\varphi, \vartheta\}$

$$\boldsymbol{c}(\varphi, \vartheta) = \cos(\varphi)\sin(\vartheta)\boldsymbol{e}_1 + \sin(\varphi)\sin(\vartheta)\boldsymbol{e}_2 + \cos(\vartheta)\boldsymbol{e}_3. \tag{8}$$

Choosing $\bar{\boldsymbol{c}} = \boldsymbol{e}_3$ and taking into account that the surface element on the unit sphere is equal to $\mathrm{d}c = \sin(\vartheta)\,\mathrm{d}\varphi\,\mathrm{d}\vartheta/(4\pi)$, the density f_ϑ of the angle ϑ is given by

$$f_\vartheta = \frac{\kappa}{2\sinh(\kappa)}\exp\left(\kappa\cos(\vartheta)\right)\sin(\vartheta), \qquad \vartheta \in [0, \pi].$$

Discrete Fisher distributions can be simulated based on this density by taking into account that the angle φ is uniformly distributed in the interval $[0, 2\pi)$ and by discretizing (2) in sets of equal-sized integrals. Fig. 2 shows pole figures of the $\boldsymbol{c}$-vector distribution for the concentration parameters $\kappa = 0.1, 1, 10, 100$ for 10000 single orientations.
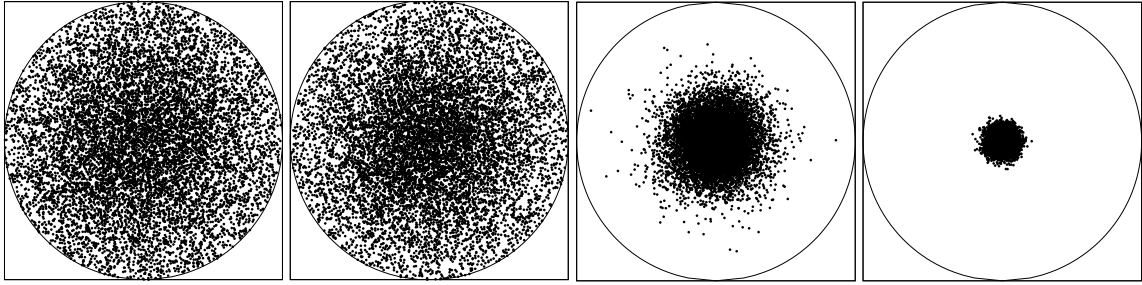

Figure 2: Stereographic projection of discrete Fisher distributions of $\boldsymbol{c}$ axes with $\kappa = 0.1, 1, 10, 100$ (from left to right) with 10000 single orientations

The definition of the terminology for the texture of pyrolytic carbon according to Reznik and Hüttinger (2002) is based on SAED measurements of the orientation angle. Additionally, the correlation between the orientation angle and the full width half maximum value (FWHM) of a distribution is used. For the Gauss distribution, for any value of the variance σ, the full width at half maximum can be defined. For $\sigma \to 0$, one asymptotically obtains a Dirac measure and the full width at half maximum is formally not defined. In the limit case of $\sigma \to \infty$, the Gauss distribution asymptotically approximates the uniform distribution for which no full width at half maximum is formally defined either. Using however Fisher distributions, one finds that a FWHM is only defined for $\kappa \geq (\ln 2)/2$, i.e. for a finite value of the concentration parameter no FWHM exists. Nevertheless, the full range of positive values of the concentration parameter κ is meaningful. Thus it is not directly possible to present values for the concentration parameter κ for describing HT, MT or LT pyrolytic carbon. Also a relation between κ and the values of the orientation angles at the boundaries, i.e. at $80°$ for the boundary between HT and MT and $50°$ between MT and LT, is not accessible.

Tensorial representation of the ODF. In the following we use the function $f(\boldsymbol{Q})$ instead of $f_c(\boldsymbol{c})$. If it is assumed that the ODF is square integrable, then there exists a tensorial Fourier expansion of the ODF. The Fourier expansion has the following general form

$$f(\boldsymbol{Q}) = 1 + \sum_{i=1}^{\infty} f_{\alpha_i}(\boldsymbol{Q}), \qquad f_{\alpha_i} = \mathbb{V}'_{\langle\alpha_i\rangle} \cdot \mathbb{F}'_{\langle\alpha_i\rangle}(\boldsymbol{Q}), \quad \mathbb{F}'_{\langle\alpha_i\rangle}(\boldsymbol{Q}) = \boldsymbol{Q} \star \mathbb{T}'_{\langle\alpha_i\rangle} \tag{9}$$

with $\{\alpha_i\} = \{2, 4, 6, \ldots\}$. The $\mathbb{V}'_{\langle\alpha_i\rangle}$ are called tensorial Fourier coefficients or texture coefficients. The bracket in subscript $\langle\cdot\rangle$ indicates the tensor rank. The tensors $\mathbb{T}'_{\langle\alpha_i\rangle}$ are called reference tensors which are normalized without loss of generality

$$\|\mathbb{T}'_{\langle\alpha_i\rangle}\| = 2\alpha + 1. \tag{10}$$

The $\mathbb{V}'_{\langle\alpha_i\rangle}$ and $\mathbb{T}'_{\langle\alpha_i\rangle}$ are completely symmetric and traceless tensors. Therefore, the following relations hold, e.g., for $\boldsymbol{V}' = \boldsymbol{V}'_{\langle 2\rangle}$ and $\mathbb{V}' = \mathbb{V}'_{\langle 4\rangle}$

$$V'_{ij} = V'_{ji}, \quad V'_{ii} = 0, \qquad V'_{ijkl} = V'_{jikl} = V'_{klij} = V'_{kjil} = \ldots, \quad V'_{iikl} = 0. \tag{11}$$

The symmetry properties of the ODF imply that the reference tensors $\mathbb{T}'_{\langle\alpha_i\rangle}$ reflect the material symmetry of the domains, i.e.,

$$\mathbb{T}'_{\langle\alpha_i\rangle} = \boldsymbol{H}^D \star \mathbb{T}'_{\langle\alpha_i\rangle} \quad \forall \boldsymbol{H}^D \in S^D, \tag{12}$$

346

whereas the tensorial Fourier coefficients $\mathbb{V}'_{\langle\alpha_i\rangle}$ have the symmetry of the microstructure

$$\mathbb{V}'_{\langle\alpha_i\rangle} = \boldsymbol{H}^M \star \mathbb{V}'_{\langle\alpha_i\rangle} \quad \forall \boldsymbol{H}^M \in S^M. \tag{13}$$

For the special case of a cubic crystal symmetry, this expansion has been used by several authors (Adams et al., 1992; Guidi et al., 1992; Böhlke, 2005, 2006).

For the homogenization of linear elastic properties, the 2nd- and 4th-order texture coefficients are of special interest. These can be derived based on elementary algebraic considerations. In the case of a single component texture, the irreducible tensors satisfy $\|\boldsymbol{V}'_{\langle2\rangle}\| = 1$ and $\|\mathbb{V}'_{\langle4\rangle}\| = 1$. Furthermore, the sample symmetry is equal to the material symmetry of the domains, i.e., they have a transversely isotropic symmetry. For these two coefficients it can be concluded that there are only two irreducible tensors which satisfy the two restrictions

$$\tilde{\boldsymbol{V}}'_{\langle2\rangle} = \frac{\sqrt{6}}{6}\begin{bmatrix} 1 & 0 & 0 \\ & 1 & 0 \\ \text{sym.} & & -2 \end{bmatrix}\boldsymbol{e}_i \otimes \boldsymbol{e}_j, \qquad \tilde{\mathbb{V}}'_{\langle4\rangle} = \frac{\sqrt{280}}{280}\begin{bmatrix} 3 & 1 & -4 & 0 & 0 & 0 \\ & 3 & -4 & 0 & 0 & 0 \\ & & 8 & 0 & 0 & 0 \\ & & & -8 & 0 & 0 \\ \text{sym.} & & & & -8 & 0 \\ & & & & & 2 \end{bmatrix}\boldsymbol{B}_\alpha \otimes \boldsymbol{B}_\beta.$$

Here, $\boldsymbol{e}_3$ is the anisotropy direction and $\{\boldsymbol{B}_\alpha\}$ represents an orthonormal basis on the space of symmetric 2nd-order tensors

$$\begin{aligned}
\boldsymbol{B}_1 &= \boldsymbol{e}_1 \otimes \boldsymbol{e}_1, & \boldsymbol{B}_4 &= \tfrac{\sqrt{2}}{2}\left(\boldsymbol{e}_2 \otimes \boldsymbol{e}_3 + \boldsymbol{e}_3 \otimes \boldsymbol{e}_2\right), \\
\boldsymbol{B}_2 &= \boldsymbol{e}_2 \otimes \boldsymbol{e}_2, & \boldsymbol{B}_5 &= \tfrac{\sqrt{2}}{2}\left(\boldsymbol{e}_1 \otimes \boldsymbol{e}_3 + \boldsymbol{e}_3 \otimes \boldsymbol{e}_1\right), \\
\boldsymbol{B}_3 &= \boldsymbol{e}_3 \otimes \boldsymbol{e}_3, & \boldsymbol{B}_6 &= \tfrac{\sqrt{2}}{2}\left(\boldsymbol{e}_1 \otimes \boldsymbol{e}_2 + \boldsymbol{e}_2 \otimes \boldsymbol{e}_1\right).
\end{aligned} \tag{14}$$

The texture coefficients of the aggregate are then given by orientation averaging

$$\boldsymbol{V}'_{\langle2\rangle} = \int_{SO(3)} f(\boldsymbol{Q})\boldsymbol{Q} \star \tilde{\boldsymbol{V}}'_{\langle2\rangle} \,\mathrm{d}Q, \qquad \mathbb{V}'_{\langle4\rangle} = \int_{SO(3)} f(\boldsymbol{Q})\boldsymbol{Q} \star \tilde{\mathbb{V}}'_{\langle4\rangle} \,\mathrm{d}Q. \tag{15}$$

3 Effective elastic properties

Elastic properties of the domains. It is possible to decompose the 4th-order elasticity tensors of arbitrary symmetry into a direct sum of orthogonal subspaces on which the action of $SO(3)$ is irreducible. The action of $SO(3)$ on a vector space is said to be irreducible if there are no proper invariant subspaces. For the stiffness tensor the harmonic decomposition has the form

$$\mathbb{C} = h_1\mathbb{P}_1^I + h_2\mathbb{P}_2^I + \boldsymbol{H}'_1 \otimes \boldsymbol{I} + \boldsymbol{I} \otimes \boldsymbol{H}'_1 + 4\mathbb{J}[\boldsymbol{H}'_2] + \mathbb{H}', \tag{16}$$

with the isotropic projectors

$$\mathbb{P}_1^I = \frac{1}{3}\boldsymbol{I} \otimes \boldsymbol{I}, \quad \mathbb{P}_2^I = \mathbb{I}^{\mathsf{S}} - \mathbb{P}_1^I, \tag{17}$$

and

$$4\mathbb{J}[\boldsymbol{A}] = \boldsymbol{A}\square\boldsymbol{I} + (\boldsymbol{A}\square\boldsymbol{I})^{\mathsf{T_R}} + \boldsymbol{I}\square\boldsymbol{A}^{\mathsf{T}} + (\boldsymbol{I}\square\boldsymbol{A}^{\mathsf{T}})^{\mathsf{T_R}} \tag{18}$$

A review concerning this representation is given by Forte and Vianello (1996). h_1 and h_2 are called the first and second isotropic parts; $\boldsymbol{H}'_1$ and $\boldsymbol{H}'_2$ are the first and the second deviatoric parts, respectively; $\mathbb{H}'$ is the harmonic part. The tensors $\boldsymbol{H}'_1$, $\boldsymbol{H}'_2$, and $\mathbb{H}'$ are irreducible, i.e., completely symmetric and traceless.

Due to the properties of the harmonic decomposition for transversely isotropic materials, the stiffness tensor can be represented immediately by

$$\mathbb{C}(\boldsymbol{Q}) = \boldsymbol{Q} \star \tilde{\mathbb{C}} = \boldsymbol{Q} \star \left(h_1\mathbb{P}_1^I + h_2\mathbb{P}_2^I + h_3(\tilde{\boldsymbol{V}}'_{\langle2\rangle} \otimes \boldsymbol{I} + \boldsymbol{I} \otimes \tilde{\boldsymbol{V}}'_{\langle2\rangle}) + 4h_4\mathbb{J}[\tilde{\boldsymbol{V}}'_{\langle2\rangle}] + h_5\tilde{\mathbb{V}}'_{\langle4\rangle}\right). \tag{19}$$

It is well known that the stiffness tensor has five independent elastic constants in the transversely isotropic case if the material is hyperelastic. In equation (19) the five parameters are given by $\{h_1, \ldots, h_5\}$. h_1 and h_2 represent the isotropic part of the stiffness tensor, h_3, h_4, h_5 the anisotropic part. For a standard orientation $\boldsymbol{Q} = \boldsymbol{I}$, the parameters $\{h_1, \ldots, h_5\}$ can be identified in terms of the components $\tilde{C}_{ijkl}$ of $\tilde{\mathbb{C}}$ being the reference stiffness with anisotropy direction equal to $\boldsymbol{e}_3$

$$h_1 = \frac{1}{3}(2\tilde{C}_{1111} + 2\tilde{C}_{1122} + 4\tilde{C}_{1133} + \tilde{C}_{3333}), \tag{20}$$

$$h_2 = \frac{1}{15}(7\tilde{C}_{1111} - 5\tilde{C}_{1122} + 2(-2\tilde{C}_{1133} + \tilde{C}_{3333} + 6\tilde{C}_{2323})), \tag{21}$$

$$h_3 = -\frac{1}{21}(\tilde{C}_{1111} - 7\tilde{C}_{1122} + 5\tilde{C}_{1133} + \tilde{C}_{3333} - 4\tilde{C}_{2323}), \tag{22}$$

$$h_4 = \frac{1}{21}(5\tilde{C}_{1111} - 7\tilde{C}_{1122} + 4\tilde{C}_{1133} - 2\tilde{C}_{3333} - 6\tilde{C}_{2323}), \tag{23}$$

$$h_5 = \frac{1}{35}(\tilde{C}_{1111} - 2\tilde{C}_{1133} + \tilde{C}_{3333} - 4\tilde{C}_{2323}). \tag{24}$$

Simple bounds. The most simple bounds are the arithmetic and harmonic mean of the local stiffness tensors, which were first suggested by Voigt and Reuss. For isotropic microstructures, where the domains differ only with respect to their orientation, these bounds can be written as

$$\mathbb{C}^V = \int_{SO(3)} f(\boldsymbol{Q})\mathbb{C}(\boldsymbol{Q})\,\mathrm{d}Q = \int_{SO(3)} f(\boldsymbol{Q})\boldsymbol{Q} \star \tilde{\mathbb{C}}\,\mathrm{d}Q \tag{25}$$

and

$$\mathbb{S}^R = \int_{SO(3)} f(\boldsymbol{Q})\mathbb{S}(\boldsymbol{Q})\,\mathrm{d}Q = \int_{SO(3)} f(\boldsymbol{Q})\boldsymbol{Q} \star \tilde{\mathbb{S}}\,\mathrm{d}Q. \tag{26}$$

Here, $\tilde{\mathbb{C}}$ and $\tilde{\mathbb{S}}$ denote the stiffness and compliance tensor of a reference domain, respectively. The arithmetic and harmonic mean correspond to the assumption of homogeneous strain and stress fields, respectively. These approaches give upper and lower bounds for the strain energy density. They represent the best bounds if the orientation distribution is the only microstructural information available.

As a consequence of the fact that the simple bounds $\mathbb{C}^V$ and $\mathbb{S}^R$ are orientation averages of $\mathbb{C}(\boldsymbol{Q})$ and $\mathbb{S}(\boldsymbol{Q})$ and that similarly $\boldsymbol{V}'_{\langle 2 \rangle}$ and $\mathbb{V}'_{\langle 4 \rangle}$ are orientation averages of $\boldsymbol{Q} \star \tilde{\boldsymbol{V}}'_{\langle 2 \rangle}$ and $\boldsymbol{Q} \star \tilde{\mathbb{V}}'_{\langle 4 \rangle}$, the following representations are valid (Böhlke et al., 2009)

$$\mathbb{C}^V = h_1\mathbb{P}_1^I + h_2\mathbb{P}_2^I + h_3(\boldsymbol{V}'_{\langle 2 \rangle} \otimes \boldsymbol{I} + \boldsymbol{I} \otimes \boldsymbol{V}'_{\langle 2 \rangle}) + h_4\mathbb{J}[\boldsymbol{V}'_{\langle 2 \rangle}] + h_5\mathbb{V}'_{\langle 4 \rangle}, \tag{27}$$

$$\mathbb{S}^R = \tilde{h}_1\mathbb{P}_1^I + \tilde{h}_2\mathbb{P}_2^I + \tilde{h}_3(\boldsymbol{V}'_{\langle 2 \rangle} \otimes \boldsymbol{I} + \boldsymbol{I} \otimes \boldsymbol{V}'_{\langle 2 \rangle}) + \tilde{h}_4\mathbb{J}[\boldsymbol{V}'_{\langle 2 \rangle}] + \tilde{h}_5\mathbb{V}'_{\langle 4 \rangle}. \tag{28}$$

The quantities $\{\tilde{h}_1, \ldots, \tilde{h}_5\}$ are defined similarly to (20)-(24) in terms of the components of the compliance tensor $\tilde{\mathbb{S}}$ of a reference domain. The stiffness tensors can be varied by changing the five elastic constants of the transversely isotropic domains and the five plus nine independent components of the texture coefficients of 2nd and 4th order.

Singular approximation. Since the simple bounds are generally rather inaccurate, we consider in the following a more precise estimate, the singular approximation (Fokin, 1972, 1973; Böhlke et al., 2010). Based on Green's function and a comparison material with stiffness $\mathbb{C}_0$, the local strain field in a heterogeneous material that is statistically homogeneous can be expressed by

$$\boldsymbol{\varepsilon} = \boldsymbol{\varepsilon}_0 - \mathcal{P}\delta\mathbb{C}[\boldsymbol{\varepsilon}] \tag{29}$$

with $\delta\mathbb{C} = \mathbb{C} - \mathbb{C}_0$ and the integral operator

$$(\mathcal{P}\delta\mathbb{C}[\boldsymbol{\varepsilon}])_{ij} = \int_{V'} \frac{\partial^2 G_{i)k}(\boldsymbol{x} - \boldsymbol{x}')}{\partial x_l' \partial x_{(j}}(\delta\mathbb{C}(\boldsymbol{x}')[\boldsymbol{\varepsilon}(\boldsymbol{x}')])_{kl}\,\mathrm{d}V' = -\int_{V'}(\mathbb{G}(\boldsymbol{x}' - \boldsymbol{x})\delta\mathbb{C}(\boldsymbol{x}')[\boldsymbol{\varepsilon}(\boldsymbol{x}')])_{ij}\,\mathrm{d}V', \tag{30}$$

where a bracket accompanying indices denotes symmetrization. G_{ik} is a Green's function in an infinite body. This integral operator is identical to the one introduced by Dederichs and Zeller (1973) and by Willis (1977) for statistically homogeneous materials. The general property of the 4th-order tensor $\mathbb{G}$ (Dederichs and Zeller, 1973; Torquato, 2002) is that it can be decomposed into a singular and a nonlocal part

$$\mathbb{G}(\boldsymbol{r}) = \mathbb{G}_0\delta(\boldsymbol{r}) + \mathbb{G}_1(\boldsymbol{r}). \tag{31}$$

Here, $\delta(\boldsymbol{r})$ is the Dirac distribution. $\mathbb{G}_0$ is a constant tensor, i.e., microstructure independent. The nonlocal part has the property $\mathbb{G}_1(\alpha\boldsymbol{r}) = \alpha^{-3}\mathbb{G}_1(\boldsymbol{r})$. The singular approximation of $\mathbb{G}$ is obtained by neglecting the nonlocal part of $\mathbb{G}$

$$\mathbb{G}(\boldsymbol{r}) \approx \mathbb{G}_0\delta(\boldsymbol{r}). \tag{32}$$

Since the nonlocal part of the integral operator is neglected, morphologic anisotropies cannot be taken into account by the singular approximation.

By eliminating the comparison strain ε_0 in (29), the strain localization relation can be derived explicitly for the phase-average of strain

$$\boldsymbol{\varepsilon} = \mathbb{A}[\bar{\boldsymbol{\varepsilon}}], \qquad \mathbb{A} = \mathbb{Y}\langle\mathbb{Y}\rangle^{-1}, \qquad \mathbb{Y} = (\mathbb{P}_0^{-1} + \delta\mathbb{C})^{-1} \tag{33}$$

with the effective strain $\bar{\varepsilon}$, the phase average of the strain localization tensor $\mathbb{A}$ and $\mathbb{P}_0 = -\mathbb{G}_0$. The effective stiffness tensor $\mathbb{C}^S$ of the singular approximation is given by

$$\mathbb{C}^S = \langle\mathbb{C}\mathbb{A}\rangle. \tag{34}$$

If an isotropic comparison medium with eigenvalues c_1 and c_2 is chosen

$$\mathbb{C}_0 = c_1\mathbb{P}_1^I + c_2\mathbb{P}_2^I, \tag{35}$$

then $\mathbb{P}_0$ is given by (see, e.g., Dederichs and Zeller, 1973)

$$\mathbb{P}_0 = p_1\mathbb{P}_1^I + p_2\mathbb{P}_2^I, \qquad p_1 = \frac{1}{c_1 + 2c_2}, \qquad p_2 = \frac{2}{5c_2}\frac{c_1 + 3c_2}{c_1 + 2c_2}. \tag{36}$$

A specific property of the singular approximation is that it is self-consistent in the sense that $\mathbb{C}^S$ and $\mathbb{S}^S$ are reciprocal $\mathbb{S}^S = (\mathbb{C}^S)^{-1}$. In the following, we specify the reference material $\mathbb{C}_0$ by the isotropic geometric mean (see, e.g., Böhlke and Bertram (2001)), i.e., for $f(\boldsymbol{Q}) = 1$. The isotropic geometric mean is given by

$$c_1 = \exp\left(\ln(\tilde{\mathbb{C}}) \cdot \mathbb{P}_1^I\right), \qquad c_2 = \exp\left(\frac{1}{5}\ln(\tilde{\mathbb{C}}) \cdot \mathbb{P}_2^I\right). \tag{37}$$

If the non-local part of the integral operator is not neglected, it is a helpful assumption that the stress polarizations are constant within each domain (Willis, 1977). For spherical inclusions, i.e. isotropic two-point statistics, $\mathbb{P}_0$ is given by

$$\mathbb{P}_0(\mathbb{C}_0) = \frac{1}{4\pi}\int_{\|\boldsymbol{n}\|=1}\mathbb{H}(\mathbb{C}_0, \boldsymbol{n})\, \mathrm{d}n \tag{38}$$

with $\mathbb{H} = \mathbb{I}^S(\boldsymbol{N}\square(\boldsymbol{n}\otimes\boldsymbol{n}))\mathbb{I}^S$, $\boldsymbol{N} = \boldsymbol{K}^{-1}$ and $\boldsymbol{K} = \mathbb{C}_0[[\boldsymbol{n}\otimes\boldsymbol{n}]]$. Based on $\bar{\mathbb{C}} = \langle\mathbb{C}\mathbb{Y}\rangle\langle\mathbb{Y}\rangle^{-1}$ and $\mathbb{Y} = (\mathbb{P}_0^{-1} + \delta\mathbb{C})^{-1}$ with $\mathbb{P}_0 = \mathbb{P}_0(\bar{\mathbb{C}})$ a self-consistent scheme is established.

4 Numerical results

The following elastic constants are taken for the domains with transversely isotropic material symmetry $\tilde{C}_{1111} = 40.016$, $\tilde{C}_{3333} = 18.185$, $\tilde{C}_{1122} = 20.021$, $\tilde{C}_{1133} = 12.779$, $\tilde{C}_{2323} = 1.776$ [GPa] which were determined by ultrasound phase spectroscopy for a highly textured PyC sample (Gebert and Wanner, 2009). Fig. 3 shows the directional dependence of Young's modulus of PyC. It is obvious that the anisotropy is significant.

Due to the rotational symmetry of the Fisher distributions, the effective response of the micro textured volume element is also of transversely isotropic symmetry. Fig. 4 (left) shows the five independent components of the stiffness tensor vs. $\lambda = 1/(1 + \kappa)$ estimated by the singular approximation. For $\lambda = 0$ one has a single domain orientation. The stiffness components then correspond to the one of the single domain stiffness tensor. For $\lambda = 1$ a uniform, i.e. isotropic texture, is obtained.

In Fig. 4 (right), the Frobenius norm of the two texture coefficients $\boldsymbol{V}'_{\langle2\rangle}$ and $\mathbb{V}'_{\langle4\rangle}$ is shown vs. λ. The norm of the coefficients is equal to zero for uniform distribution and equal to one for single orientation distributions. Otherwise, the norm is in the interval $(0, 1)$. Hence, the norms are natural measures of anisotropy with respect to these two moment tensors. In the figure it can be seen that there is a rapid decrease of anisotropy with increasing λ. Lines connecting the points are given only for better visibility.
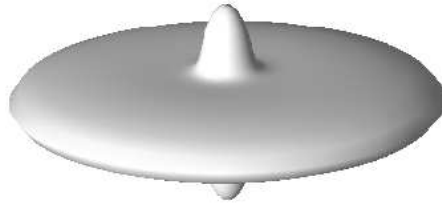
Figure 3: Graphical representation of the directional dependence of Young's modulus of PyC, where the vertical axis corresponds to the c-axis
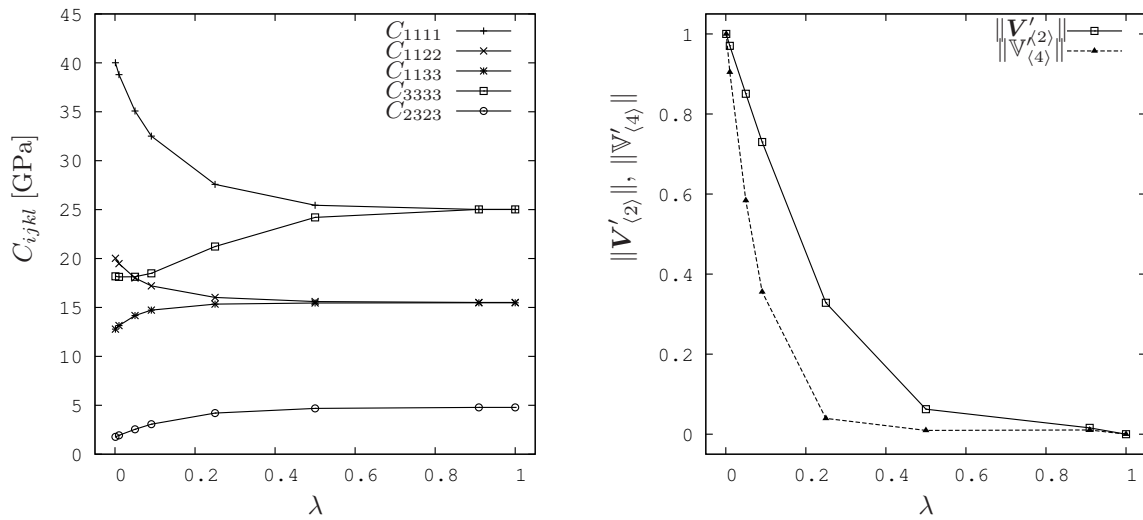

Figure 4: Components of the effective elasticity tensor obtained by the singular approximation vs. the concentration parameter $\lambda = 1/(1 + \kappa)$ (left). Norm of the texture coefficients $\boldsymbol{V}'_{\langle 2 \rangle}$ and $\mathbb{V}'_{\langle 4 \rangle}$ vs. λ (right).
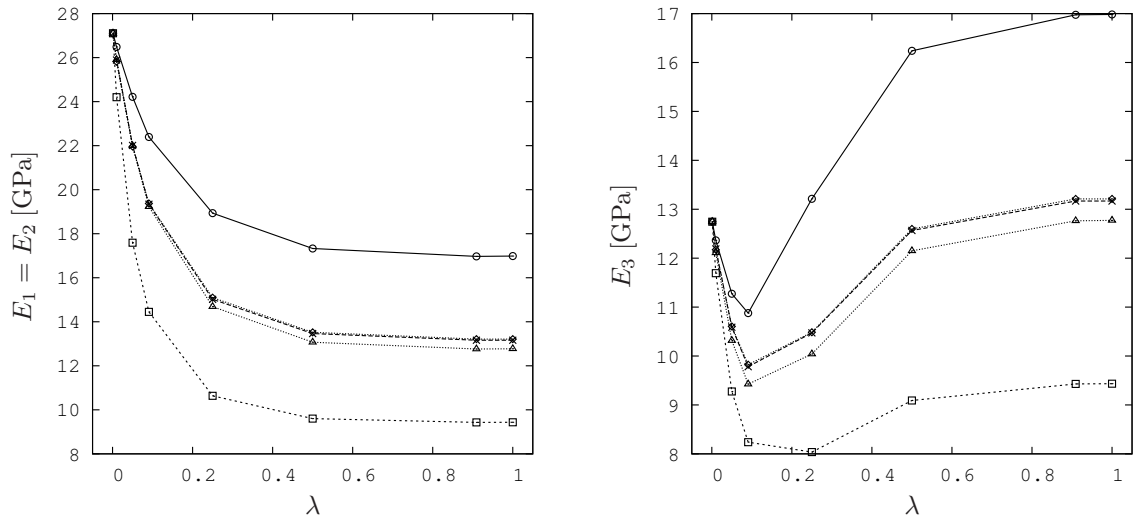

Figure 5: Voigt bound ($\circ$), Reuss bound ($\square$), singular approximation ($\times$), geometric mean ($\triangle$) and self-consistent estimate ($\diamond$) of Young's modulus in the plane of isotropy (left) and in the direction of average c-axis (right) vs. $\lambda(\kappa)$.

Fig. 5 shows the two independent values of Young's modulus vs. λ for the simple bounds, the geometric mean, the singular approximation and the self-consistent estimate. For the single component texture, i.e. $\lambda = 0$, all estimates coincide.

It is obvious that between the simple bounds there is a significant gap even for small values of λ which implies that these bounds are not appropriate for estimating the effective properties. In the range between the bounds morphologic aspects of the microstructure determine the precise values of the effective properties. Furthermore, it can be seen that the singular approximation is very close to the self-consistent estimate. Also the difference between the geometric mean and the singular approximation is small. Similar conclusions can be deduced for the values of the shear modulus given in Fig. 6.

Young's modulus in direction of $\bar{c} = e_3$ shows an interesting behavior, i.e., firstly it decreases with increasing λ up to a minimum value and then it increases. This specific behavior can be explained by Fig. 3, since a path on the surface of the body of Young's modulus from the c-axes to the isotropic plane shows a similar curve.
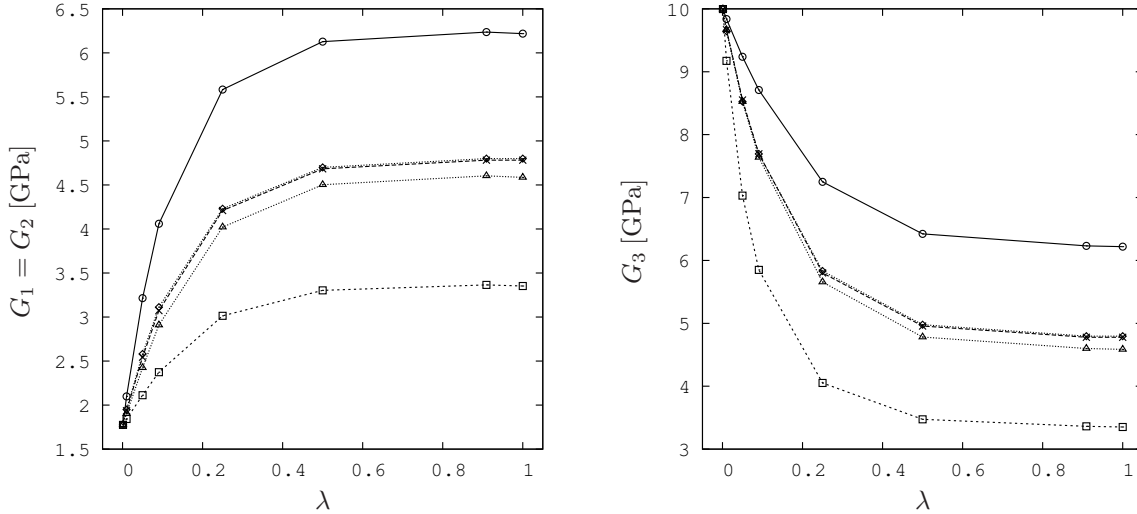

Figure 6: Voigt bound ($\circ$), Reuss bound ($\square$), singular approximation ($\times$), geometric mean ($\triangle$) and self-consistent estimate ($\diamond$) of the shear modulus in the plane of isotropy (left) and in the direction of average c-axis (right) vs. $\lambda(\kappa)$.

Taylor et al. (2003) provided nanoindentation tests (Berkovich indenter) perpendicular to deposition direction on HT PyC films and measured values of Young's modulus between 16.1 and 26.2 GPa. These values are in good agreement to the calculated elastic moduli for small values of λ which corresponds to highly-textured PyC (see Fig. 5 left). Guellali et al. (2008a) determined the elastic properties of highly textured PyC layers deposited on plane substrates via micro indentation tests. The measured value of Young's modulus is 15.5 GPa for HT PyC and is close to the calculated values for small λ using the singular approximation, the geometric mean and the self-consistent estimate. The comparison with the rare experimental data shows that numerical results obtained give reasonable estimates of the elastic properties on the submicron scale.

5   Summary and conclusions

In the present paper, the orientation dependence of the stiffness tensor of PyC on the micrometer scale has been determined based on the elastic properties of the domains and the orientation distribution of the domains. A Fisher distribution function has been used as a texture component model, which is a one-parameter orientation distribution function. The effective elastic properties on the micrometer scale have been determined based on simple bounds, the geometric mean, the singular approximation and the self-consistent estimate.

The numerical results indicate that the strong elastic anisotropy of PyC induces a large gap between the simple bounds. Furthermore, it is found that the singular approximation, geometric mean and the self-consistent estimate give very similar values for the effective elasticities. Compared to the geometric mean the singular approximation is based on clear micromechanical assumptions. The determination of the singular approximation is much simpler compared to the self-consistent estimate. It can be concluded that for approximately spherical domains, the singular approximation is preferable.

The bounds and the approximations of the effective elastic properties depend only on one concentration parameter which completely specifies the Fisher distributions. More micromechanical investigations have to be carried out

in order to better understand how the concentration parameter of the Fisher distribution of the normal vectors on the graphene planes can be used to classify the texture degrees of pyrolytic carbon. Still Fig. 5 and 6 indicate that there are significant gradients in the elastic properties of the material throughout the whole domain of the values for λ and thus throughout the different texture degrees HT, MT and LT.

References

Adams, B.; Boehler, J.; Guidi, M.; Onat, E.: Group theory and representation of microstructure and mechanical behavior of polycrystals. *J. Mech. Phys. Solids*, 40, 4, (1992), 723–737.

Böhlke, T.: Application of the maximum entropy method in texture analysis. *Comp. Mat. Sc.*, 32, (2005), 276–283.

Böhlke, T.: Texture simulation based on tensorial fourier coefficients. *Comp. Struct.*, 84, (2006), 1086–1094.

Böhlke, T.; Bertram, A.: The evolution of Hooke's law due to texture development in polycrystals. *Int. J. Solids Struct.*, 38, 52, (2001), 9437–9459.

Böhlke, T.; Jöchen, K.; Kraft, O.; Löhe, D.; Schulze, V.: Elastic properties of polycrystalline microcomponents. *Mechanics of Materials*, 42, (2010), 11–23.

Böhlke, T.; Langhoff, T.-A.; Piat, R.: Bounds for the elastic properties of pyrolytic carbon. *PAMM*, 9, (2009), 431–434.

Bunge, H.-J.: *Texture Analysis in Materials Science*. Cuvillier Verlag Göttingen (1993).

Dederichs, P. H.; Zeller, R.: Variational treatment of the elastic constants of disordered materials. *Z. Physik A*, 259, (1973), 103–116.

Diss, P.; Lamon, J.; Carpentier, L.; Loubet, J.; Kapsa, P.: Sharp indentation behavior of carbon/carbon composites and varieties of carbon. *Carbon*, 40, 14, (2002), 2567–2579.

Fisher, R.: Dispersion on a sphere. *Proc. Roy. Soc. London Ser. A*, 217, (1953), 295–305.

Fitzer, E.; Manocha, L.: *Carbon Reinforcements and Carbon/Carbon Composites*. Springer (1998).

Fokin, A. G.: Solution of statistical problems in elasticity theory in the singular approximation. *Journal of Applied Mechanics and Technical Physics*, 13, (1972), 85–89.

Fokin, A. G.: Singular approximation for the calculation of the elastic properties of reinforced systems. *Mech. Compos. Mater.*, 9, 3, (1973), 445–449.

Forte, S.; Vianello, M.: Symmetry classes for elasticity tensors. *J. Elast.*, 43, (1996), 81–108.

Gebert, J.-M.; Wanner, A.: *Private communications*. Institut für Werkstoffkunde I, Karlsruhe Institute of Technology (2009).

Guellali, M.; Oberacker, R.; Hoffmann, M.: Influence of heat treatment on microstructure and mechanical properties of cvi-cfc composites with medium and highly textured pyrocarbon matrices. *Composite Science and Technology*, 68, 5, (2008a), 1115–1121.

Guellali, M.; Oberacker, R.; Hoffmann, M.: Influence of heat treatment on microstructure and properties of highly textured pyrocarbons deposited during CVD at about 1100°C and above 2000°C. *Composite Science and Technology*, 68, 5, (2008b), 1122–1130.

Guidi, M.; Adams, B.; Onat, E.: Tensorial representation of the orientation distribution function in cubic polycrystals. *Textures Microstruct.*, 19, (1992), 147–167.

Herbell, T.; Eckel, A.: Ceramics for rocket engine components. *Aerospace Engineering*, 11, 12, (1991), 21–23.

Kocks, U.; Tome, C.; Wenk, H.: *Texture and Anisotropy: Preferred Orientations in Polycrystals and Their Effect on Materials Properties*. Cambridge Univ. Pr. (1998).

Papadakis, E. P.; Bernstein, H.: Elastic moduli of pyrolytic graphite. *J of the Acoustical Sci. of America.*, 35, 4, (1963), 521–524.

Piat, R.; Reznik, B.; Schnack, E.; Gerthsen, D.: Modeling of effective material properties of carbon fibers and CVI matrices. *Composite Science and Technology*, 64, 13-14, (2004), 2015–2020.

Reznik, B.; Gerthsen, D.; Hüttinger, K.: Micro- and nanostructure of the carbon matrix of infiltrated carbon fiber felts. *Carbon*, 39, 2, (2001), 215–219.

Reznik, B.; Gerthsen, D.; Zhang, W.; Hüttinger, K.: Texture changes in the matrix of an infiltrated in a carbon fiber felt studied by polarized light microscopy and selected area electron diffraction. *Carbon*, 41, 2, (2003), 376–380.

Reznik, B.; Hüttinger, K.: On the terminology for pyrolytic carbon. *Carbon*, 40, 4, (2002), 621–24.

Sauder, C.; Lamon, J.: Prediction of elastic properties of carbon fibers and CVI matrices. *Carbon*, 43, 10, (2005), 2044–2053.

Sauder, C.; Lamon, J.; Pailler, R.: The tensile properties of carbon matrices at temperatures uo to 2200°. *Carbon*, 43, 10, (2005), 2054–2065.

Schaeben, H.: Parametrization and probability distributions of orientations. *Textures and Microstructures*, 13, (1990), 51–54.

Schaeben, H.: "Normal" orientation distribution. *Textures and Microstructures*, 19, (1992), 197–202.

Taylor, C.; Wayne, W.; Chiu, W.: Residual stress measurement in thin carbon films by raman spectroscopy and nanoindentation. 429(1-2), (2003), 190–200.

Torquato, S.: *Random Heterogeneous Materials: Microstructures and Macroscopic Properties*. Springer (2002).

Willis, J.: Bounds and self-consistent estimates for the overall properties of anisotropic composites. *J. Mech. Phys. Solids*, 25, (1977), 185–202.

Addresses: T. Böhlke, K. Jöchen, R. Piat, T.-A. Langhoff, Chair for Continuum Mechanics, Institute of Engineering Mechanics, Karlsruhe Institute of Technology (KIT), POB 6980, D-76128 Karlsruhe, Germany, email: `{boehlke,joechen,piat,langhoff}@itm.uni-karlsruhe.de`, I. Tsukrov, Mechanical Engineering Department, University of New Hampshire, email: `Igor.Tsukrov@unh.edu`, B. Reznik, Institute for Chemical Technology and Polymer Chemistry, Karlsruhe Institute of Technology (KIT), `Reznik@ict.uni-karlsruhe.de`